Computational Thermal Sciences, 6 (2): 103–111 (2014)

RADIATIVE TRANSFER IN VACUUM THERMAL INSULATION OF SPACE VEHICLES

I. V. Gritsevich,[1,] L. A. Dombrovsky,[2] & A. V. Nenarokomov[1]*

[1]*Moscow Aviation Institute, Moscow, Russia*

[2]*Joint Institute for High Temperatures, Moscow, Russia*

[*]Address all correspondence to I. V. Gritsevich E-mail: igrid@mail.ru

An improved radiative transfer model for vacuum thermal insulations of space vehicles is developed. The effects of both the fibrous spacer between the metal foils and thin oxide layer on the foil surface are taken into account in the calculations of the integral radiative flux through the insulation. Parametric calculations at realistic values of the problem parameters indicate that absorption and scattering of thermal radiation by fibers do not lead to a significant decrease in the radiative flux. At the same time, even very thin oxide films on the surfaces of aluminum foils should be taken into account in engineering calculations. Theoretical estimates show that not even a very dense spacer made of metalized glass fibers with aluminum coating about 50 nm thick may lead to almost a twofold decrease in the integral radiative flux.

KEY WORDS: *radiation, thermal insulation, fibrous spacer, oxide film, computational model, space vehicle*

1. INTRODUCTION

The present study is motivated by optimization of the so-called passive thermal control systems (TCSs) for space vehicles. The specifics of external heating of space vehicles during flight in vacuum enables us to consider some variants of a passive TCS based on screening the vehicle surface from external radiation of different natures. This may be direct solar radiation, solar radiation reflected by planets, as well as thermal radiation of closely spaced planets. Various multilayer insulations (MLIs) are widely used to solve this engineering problem (Malozemov et al., 1986). This type of vacuum insulation has obvious advantages, such as high thermal resistance at a relatively low density and convenience of use for surfaces of complex shape. It may be interesting to compare MLIs with vacuum insulation panels (VIPs) used in building applications (Fricke et al., 2008; Baetens et al., 2010; Bouquerel et al., 2012). There are some general features of MLIs and VIPs; however, space conditions lead to additional strong restrictions.

A typical MLI looks like a set of thin metal screens about 0.5–0.9 μm thick with spacers in between that prevent contact between the screens. Simple estimates show that the use of several layers (screens with spacers) may lead to a significant reduction of heat flux to the protected surface. In MLIs, 10–30 shielding layers are usually used. Various materials are used in MLI. The material choice depends on the expected temperature level. A polyethylene terephthalate (PET) film coated with aluminum, silver, or gold can be used for screens at working temperatures of MLI up to 423 K. Aluminum foil with fiberglass spacers is used at higher temperatures up to 723 K. At temperatures greater than 723 K, the foil is made of copper, nickel, or steel and the spacer is made of quartz fibers. The surface density of 10 screens of PET film is in the range of 0.2–0.3 kg/m^2, whereas the use of metal foils increases this value up to 1 kg/m^2 (Malozemov et al., 1986). However, regardless of the materials used in layers and spacers, the principle of the MLI is the same.

The MLI thermal models used in engineering calculations do not take into account the effect of spacers on heat transfer (Alifanov et al., 2009; Nenarokomov et al., 2010). To the best of our knowledge, this effect was also not considered in the literature before our recent paper (Gritsevich et al., 2013). At the same time, the desirable increase in accuracy in the calculations of a spacecraft's thermal insulation requires analysis of all potentially im-

1940–2503/14/$35.00

NOMENCLATURE

A	absorbance
a	fiber radius
B_λ	Planck function
c	specific heat capacity
d	spacer thickness
k	heat transfer coefficient
L	number of screens
l	current number of the screen
n	index of refraction
p	surface porosity
Q	efficiency factor of absorption, scattering or extinction
q	radiative flux
R	reflectance
T	temperature, transmittance
t	time
x	diffraction (size) parameter

Greek Symbols

α, θ, ψ	angles in Eq. (8)
Δ	thickness of oxide film
δ	layer thickness
ε	emittance
κ	index of absorption
λ	radiation wavelength
ρ	density
σ	Stefan–Boltzmann constant

Subscripts and Superscripts

a	absorption
b	backscattering
eff	effective
ext	external
int	internal
n	normal
R	reflected
s	scattering, solar
sp	spacer
tr	transport
λ	wavelength
1, 2	screen numbers

portant factors. This was the motivation for the present study, in which special attention is given to the effect of the radiative characteristics of fibrous spacers on heat transfer by radiation.

2. TRADITIONAL THERMAL MODEL

A simplified computational model with L opaque isothermal elements (screens) is traditionally used in approximate engineering calculations (Malozemov et al., 1986). In this model, the spacers are not considered as separate elements of MLI. Moreover, the so-called gray model is employed and the real spectral characteristics of surfaces are ignored. In this case, the mathematical model of transient heat transfer includes the following coupled ordinary differential equations:

$$\rho_1 c_1(T)\,\delta_1 \frac{dT_1}{dt} = A_s(T_1)\,[q_s(\tau) + q_R(\tau)] + \varepsilon_1(T_1) \times q_\varepsilon(\tau) - \varepsilon_1(T)\,\sigma T_1^4 + \varepsilon_{1,2}^{\text{eff}}\sigma\left(T_2^4 - T_1^4\right) + k_{1,2}(T_2 - T_1)$$

$$\rho_1 c_1(T)\,\delta_l \frac{dT_l}{dt} = \varepsilon_{l-1,l}^{\text{eff}}\sigma\left(T_{l-1}^4 - T_l^4\right) + k_{l-1,l} \times (T_{l-1} - T_l) + \varepsilon_{l,l+1}^{\text{eff}}\sigma\left(T_{l+1}^4 - T_l^4\right) + k_{l,l+1}(T_{l+1} - T_l), \quad l = 2, \ldots, L \tag{1}$$

$$\rho_L c_L(T)\,\delta_L \frac{dT_L}{dt} = \varepsilon_{L-1,L}^{\text{eff}}\sigma\left(T_{L-1}^4 - T_L^4\right) + k_{L-1,L} \times (T_{L-1} - T_L) + k_{\text{int}}(T_{\text{int}} - T_L), \quad t_{\min} < t \le t_{\max}$$

where

$$\varepsilon_{l-1,l}^{\text{eff}} = \frac{\varepsilon_{l-1}(T_{l-1})\,\varepsilon_l(T_l)}{\varepsilon_{l-1}(T_{l-1}) + \varepsilon_l(T_l) - \varepsilon_{l-1}(T_{l-1})\,\varepsilon_l(T_l)}$$

where T_l is the temperature of element number l with thickness δ_l; ρ_l, and c_l are the density and specific heat capacity of the element material; $k_{l-1,l}$ is the conventional heat transfer coefficient between elements l and $l-1$; ε_l is the integral hemispherical emittance of the element; $\varepsilon_{l-1,l}^{\text{eff}}$ is the effective integral hemispherical emittance of the system of neighboring elements; q_s is the integral (over the spectrum) solar radiative flux; q_R is the

integral flux of solar radiation reflected by a planet; q_ε is the integral flux of the planet's radiation; A_s is the average (gray) absorption coefficient for solar radiation; and k_{int} is the heat transfer coefficient between the Lth element of MLI and the protected surface of a spacecraft. To complete the above approximate thermal model, one needs not only the initial conditions but also some specific models for the components of the external radiative flux and the values of both the integral emittance and conventional heat transfer coefficients.

3. IMPROVED MODEL OF RADIATION HEAT TRANSFER

Let's consider a single element of MLI, which consists of two screens and a spacer made of semi-transparent highly porous fibrous material (see Fig. 1). The following assumptions are used in the heat transfer model: (1) the radiative flux in the normal direction can be determined as a solution of a one-dimensional problem neglecting small two-dimensional effects; (2) there is no thermal contact between the screens and spacer, and thermal radiation is the only heat transfer mode to be considered; (3) the normal emission and reflection are the most important properties of the surfaces, and the angular dependences of the radiative properties of these surfaces can be ignored; and (4) the isothermal metal screens are totally opaque for thermal radiation. It is also assumed that the so-called near-field effect in radiative heat transfer is negligible because the distance between the metal screens is not too small (Chapius et al., 2008; Kralik et al., 2012; Parka and Zhang, 2013). The latter corresponds to the vacuum flight conditions when the remaining gas between the metal screens leads to an increase in the internal gap thickness of the insulation layer. The previous assumptions enable us to use the following simple differential equations:

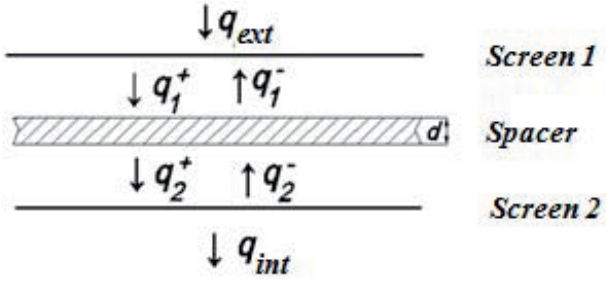

FIG. 1: Scheme of the problem

$$\begin{aligned}
\rho_1 c_1 \delta_1 \frac{dT_1}{dt} &= q_{\text{ext}} + q_1^- - q_1^+ \\
\rho_{\text{sp}} c_{\text{sp}} \delta_{\text{sp}} \frac{dT_{\text{sp}}}{dt} &= q_1^+ - q_1^- - \left(q_2^+ - q_2^-\right) \\
\rho_2 c_2 \delta_2 \frac{dT_2}{dt} &= q_2^+ - q_2^- - q_{\text{int}}
\end{aligned} \tag{2}$$

Photographs of typical spacer materials are shown in Fig. 2.

The heat capacity of each MLI layer is very small. This makes it possible to assume that a quasi-steady regime takes place in the case of slower variations in external heat transfer conditions. This approach appears to be correct in most cases. The resulting simplifications are very

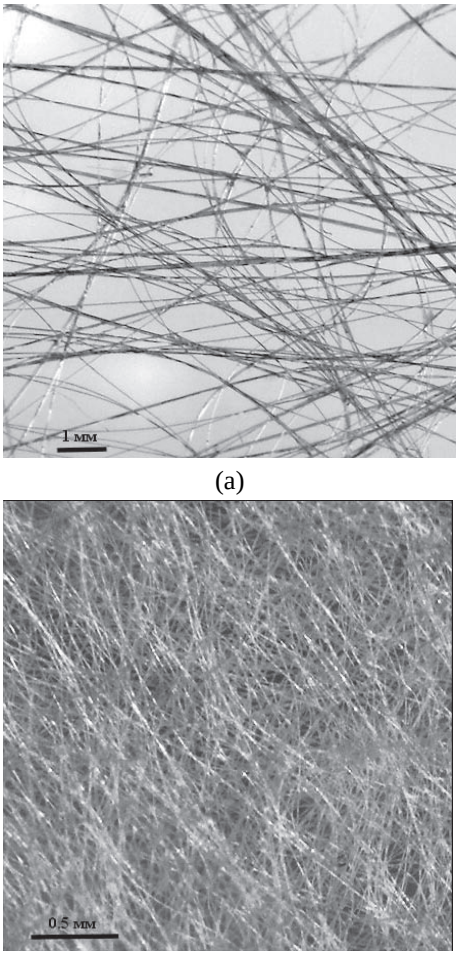

(a)

(b)

FIG. 2: Photographs of typical materials used for spacers between two foil layers: **(a)** very low-density material; **(b)** relatively dense material

important because it is sufficient to consider the following balance equations in spectral radiation fluxes:

$$\begin{aligned} q^{+}_{1,\lambda} &= \varepsilon_{1,\lambda} f_{1,\lambda} + (1-\varepsilon_{1,\lambda})\, q^{-}_{1,\lambda}, \\ q^{-}_{1,\lambda} &= \varepsilon_{\mathrm{sp},\lambda} f_{\mathrm{sp},\lambda} + R_\lambda q^{+}_{1,\lambda} + T_\lambda q^{-}_{2,\lambda}, \\ q^{+}_{2,\lambda} &= \varepsilon_{\mathrm{sp},\lambda} f_{\mathrm{sp},\lambda} + R_\lambda q^{-}_{2,\lambda} + T_\lambda q^{+}_{1,\lambda}, \\ q^{-}_{2,\lambda} &= \varepsilon_{2,\lambda} f_{2,\lambda} + (1-\varepsilon_{2,\lambda})\, q^{+}_{2,\lambda} \end{aligned} \tag{3}$$

where $q^{\pm}_{i,\lambda}$ are the spectral radiative fluxes in the gap with number i in the forward and backward hemispheres; $\varepsilon_{1,\lambda}$ and $\varepsilon_{2,\lambda}$ are the spectral hemispherical emittances of the screens at temperatures T_1 and T_2; $f_\lambda = \pi B_\lambda(T)$ is the blackbody spectral radiative flux; $B_\lambda(T)$ is the Planck function; and R_λ and T_λ are the spectral hemispherical reflectance and transmittance of the spacer. According to Kirchhoff's law, spectral hemispherical emittance of the spacer is expressed as $\varepsilon_{\mathrm{sp},\lambda} = 1 - R_\lambda - T_\lambda$.

In the case of a quasi-steady process, the resulting radiative fluxes in the two gaps are equal to each other:

$$q_\lambda = q^{+}_{1,\lambda} - q^{-}_{1,\lambda} = q^{+}_{2,\lambda} - q^{-}_{2,\lambda} \tag{4}$$

and Eqs. (3) are reduced to

$$q_\lambda = (f_{1,\lambda} - f_{2,\lambda}) \,/\, \big[1/\varepsilon_{1,\lambda} + 1/\varepsilon_{2,\lambda} + 2/\big(1 + T_\lambda - R_\lambda\big) - 2\big] \tag{5}$$

The corresponding integral radiative flux is determined as $q = \int_0^\infty q_\lambda d\lambda$. In further calculations, the aluminum foil screens and quartz fibrous spacer are considered.

4. MODELING OF OPTICAL PROPERTIES

4.1 Semi-Transparent Fibrous Spacers

Both transmittance and reflectance of radiation by highly porous fibrous spacers can be determined on the basis of the independent scattering hypothesis and Mie theory for infinite homogeneous cylinders (Bohren and Huffman, 1983; Lee and Cunnington, 1998; Dombrovsky and Baillis, 2010). One can see in Fig. 2 that typical fibrous materials used for MLI spacers are made of fibers randomly oriented in the plane of the material layer.

In the heat transfer problem, the transport efficiency factor of extinction Q_{tr}, the efficiency factor of scattering Q_{s}, and the efficiency factor of absorption Q_{a} at arbitrary illumination of fibers can be obtained by neglecting the polarization effects as follows:

$$\begin{aligned} Q_{\mathrm{s}} &= \big(Q^{\mathrm{E}}_{\mathrm{s}} + Q^{\mathrm{H}}_{\mathrm{s}}\big)/2, \quad Q_{\mathrm{tr}} = \big(Q^{\mathrm{E}}_{\mathrm{tr}} + Q^{\mathrm{H}}_{\mathrm{tr}}\big)/2, \\ Q_{\mathrm{a}} &= \big(Q^{\mathrm{E}}_{\mathrm{a}} + Q^{\mathrm{H}}_{\mathrm{a}}\big)/2 = Q_{\mathrm{tr}} - Q_{\mathrm{s}} \end{aligned} \tag{6}$$

In the case of fibers randomly oriented in parallel planes, it is convenient to use the efficiency factors averaged over the orientations (Lee 1986, 1988; Lee and Cunnington, 1998) as follows:

$$\begin{aligned} \tilde{Q}_{\mathrm{a}} &= \int_0^{\pi/2} \bar{Q}_{\mathrm{a}}(\theta) \sin(\theta)\, d\theta, \\ \tilde{Q}_{\mathrm{tr}} &= 3 \int_0^{\pi/2} \bar{Q}_{\mathrm{tr}}(\theta) \cos^2(\theta)\, d\theta, \quad \tilde{Q}^{\mathrm{tr}}_{\mathrm{s}} = \tilde{Q}_{\mathrm{tr}} - \tilde{Q}_{\mathrm{a}} \end{aligned} \tag{7}$$

where

$$\begin{aligned} &\big\{\bar{Q}_{\mathrm{tr}}(\theta), \bar{Q}^{\mathrm{tr}}_{\mathrm{s}}(\theta), \bar{Q}_{\mathrm{a}}(\theta)\big\} \\ &= \frac{1}{2\pi} \int_0^{2\pi} \big\{Q_{\mathrm{tr}}(\alpha), Q^{\mathrm{tr}}_{\mathrm{s}}(\alpha), Q_{\mathrm{a}}(\alpha)\big\}\, d\psi \end{aligned} \tag{8}$$

where $\alpha = |\arcsin[\sin(\theta)\sin(\psi)]|$ is the incidence angle for a single fiber f; θ is the incidence angle for the plane of fibers; and ψ is the angle between the plane of incidence and the normal plane (for more details, see Dombrovsky and Baillis, 2010, chapter 2). Additional information on transport approximation and the use of this approach in solving radiative transfer problems can also be found in the overview paper by Dombrovsky (2012).

The following assumptions are used to estimate both reflectance and transmittance of a fibrous spacer: the multiple scattering by fibers in a thin semi-transparent spacer can be neglected and there are no dependent scattering effects for randomly oriented fibers in a spacer. Obviously, the previous assumptions are correct in the case of a thin highly porous spacer. As a result, the following simple relationships for the absorbance and reflectance of a monodisperse layer of fibers can be used (Dombrovsky and Baillis, 2010):

$$A_\lambda = \frac{4}{\pi}(1-p)\,\tilde{Q}_{\mathrm{a}}, \quad R_\lambda = \frac{4}{\pi}(1-p)\,\tilde{Q}^{\mathrm{b}}_{\mathrm{s}} \tag{9}$$

where p is the surface porosity of a spacer; and $\tilde{Q}^{\mathrm{b}}_{\mathrm{s}} = Q^{\mathrm{tr}}_{\mathrm{s}}/2$ is the efficiency factor of backscattering.

Equation (5) shows that the mathematical model includes only the following combination of reflectance and transmittance: $U_\lambda = T_\lambda - R_\lambda$. Therefore, it is convenient to use U_λ in further analysis. Taking into account that $A_\lambda = 1 - R_\lambda - T_\lambda$, one can obtain the expression for the value of U_λ as follows:

$$U_\lambda = 1 - A_\lambda - 2R_\lambda = 1 - \frac{4}{\pi}(1-p)\,\tilde{Q}_{\mathrm{tr}} \tag{10}$$

4.2 Aluminum Foils with a Thin Oxide Layer

It is known that a thin oxide film is formed on the surface of an aluminum foil under normal atmospheric conditions. It usually takes about 2 h to form a 10-nm-thick oxide film (Bartl and Baranek, 2004). This oxide film protects bulk aluminum from further oxidation. The characteristics of oxidized aluminum foil are calculated by solving the problem illustrated schematically in Fig. 3. The resulting normal emittance is calculated as suggested in Brannon and Goldstein (1970). By using Fresnel's relationships (Born and Wolf, 1999), one can obtain the following expression for normal reflectance, taking into account the oxide film:

$$R_{\mathrm{n},\lambda}=\frac{\begin{array}{l}\left(g_1^2+h_1^2\right)\exp\left(2\mu_1\right)+\left(g_2^2+h_2^2\right)\\ \times\exp\left(-2\mu_1\right)+A\cos 2\gamma_1+B\sin 2\gamma_1\end{array}}{\begin{array}{l}e^{2\mu_1}+\left(g_1^2+h_1^2\right)\left(g_2^2+h_2^2\right)\exp\left(-2\mu_1\right)\\ +E\cos 2\gamma_1+D\sin 2\gamma_1\end{array}} \tag{11}$$

where

$$\begin{aligned}
g_1&=\frac{n_0^2-n_1^2-\kappa_1^2}{\left(n_0+n_1\right)^2+\kappa_1^2},\quad h_1=\frac{2n_0\kappa_1}{\left(n_0+n_1\right)^2+\kappa_1^2}\\
g_2&=\frac{n_1^2-n_2^2-\kappa_1^2-\kappa_2^2}{\left(n_1+n_2\right)^2+\left(\kappa_1+\kappa_2\right)^2},\\
h_2&=\frac{2\left(n_1\kappa_2-n_2\kappa_1\right)}{\left(n_1+n_2\right)^2+\left(\kappa_1+\kappa_2\right)^2}\\
\mu_1&=\frac{2\pi\kappa_1\Delta}{\lambda},\ \ \gamma_1=\frac{2\pi n_1\Delta}{\lambda},\\
A&=2(g_1g_2+h_1h_2),\quad B=2(g_1h_2-g_2h_1),\\
E&=2(g_1g_2-h_1h_2),\quad D=2(g_1h_2+g_2h_1)
\end{aligned} \tag{12}$$

According to Kirchhoff's law, the spectral normal emittance is equal to $\varepsilon_{n,\lambda} = 1 - R_{n,\lambda}$. The integral emittance is calculated as follows:

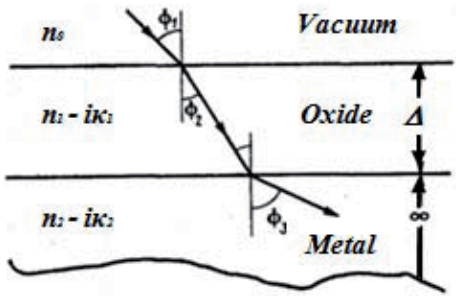

FIG. 3: Scheme of the problem for the emittance of aluminum foil coated with oxide film

$$\varepsilon_{\mathrm{n}}=\int_0^\infty \varepsilon_{\mathrm{n},\lambda}B_\lambda\left(T\right)/\sigma T^4 \tag{13}$$

Note that for polished metals, when $\varepsilon_n < 0.5$, the hemispherical emittance is slightly greater than the normal emittance (Howell et al., 2010). At the same time, the oxidation of the metal foil leads to a less pronounced angular dependence of the surface emittance. To simplify the theoretical model, taking into account the oxide film effect, we use the following approximate relationship:

$$\varepsilon_\lambda\left(\Delta\right)=\varepsilon_{\mathrm{n},\lambda}\left(\Delta\right)\frac{\varepsilon_\lambda\left(0\right)}{\varepsilon_{\mathrm{n},\lambda}\left(0\right)} \tag{14}$$

where $\varepsilon_{n,\lambda}(0)$ and $\varepsilon_\lambda(0)$ are the normal and hemispherical emittances of the non-oxidized film, respectively. The ratios of $\varepsilon_\lambda(0)/\varepsilon_{n,\lambda}(0)$ were taken from Howell et al. (2010), depending on the value of $\varepsilon_{n,\lambda}(0)$. Note that the thickness of the oxide films on both surfaces of the aluminum foil is originally the same due to manufacturing conditions, and no subsequent variation of this thickness in space is expected.

4.3 Optical Properties of Fused Silica

Infrared optical properties of fused silica have been studied for many years and the optical constants needed for calculations are well known (Kitamura et al., 2007). Fused silica has weak absorption in the short-wave range of $\lambda < 4$ μm. In the middle infrared range fused silica is opaque. Two strong absorption bands are located at wavelengths λ = 9.5 and 12.5 μm. The temperature dependence of the optical constants of fused silica is weak (Beder et al., 1971; Banner et al., 1989; Tan and Arndt, 2000), and we neglect this small effect in the calculations.

4.4 Optical Properties of Aluminum and Aluminum Oxide

The infrared optical constants of aluminum and aluminum oxide can be found in the literature (Gryvnak and Burch, 1965; Brannon and Goldstein, 1970; Whitson, 1975; Lingart et al., 1982). The index of refraction, n_λ, of aluminum oxide weakly depends on the temperature, and its spectral variation in the near-infrared range is negligible. On the contrary, the index of absorption, κ_λ, increases with the wavelength. In the far-infrared range, there are two absorption bands at λ = 18 and 23 μm, which become less pronounced at relatively high temperatures. The optical constants of aluminum increase almost linearly with

the wavelength, which is typical for metals in this group (Sokolov, 1961; Ordal et al., 1983). The temperature dependence of the optical constants of aluminum is insignificant and this effect is neglected in the present paper.

5. RESULTS OF THE CALCULATIONS

The transport efficiency factor of extinction for monodisperse quartz fibers, randomly oriented in the plane normal to the incident radiation are shown in Fig. 4. One can see that the effect of the fiber radius is not significant, at least not for fibers that are too thin. The whole spectral range can be divided into two spectral bands with quite different $\tilde{Q}_{\rm tr}$ levels. These spectral bands are $2 < \lambda < 8$ and $8 < \lambda < 12$ μm.

The results of the radiative transfer calculations for a single MLI layer at various surface porosities of the spacer and radii of the quartz fiber at realistic temperatures of T_1 = 500 K, T_2 = 300 K, and $T_{\rm sp}$ = 400 K are presented in Fig. 5. The thickness of the oxide film on the foil surface was assumed to be equal to 10 nm. The wavelength range of $1 \le \lambda \le 20$ μm was taken into account while integrating over the spectrum because the main contribution to the integral flux of thermal radiation is in this range. The effect of the semi-transparent quartz-fiber spacer appears to be insignificant even in the case of a relatively dense spacer. The minimum in curve $q(a)$ at a = 1.2 μm and p = 0.2 is explained by the Mie scattering effect.

Figure 6 indicates the considerable effect of the alumina film for one of the variants. An increase in the radiative flux with the film thickness, Δ, should be taken into account in the case of $\Delta > 0.1$ μm.

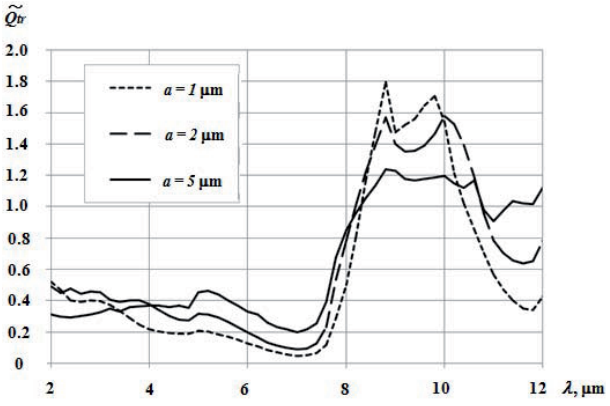

FIG. 4: Transport efficiency factor of extinction for quartz fibers

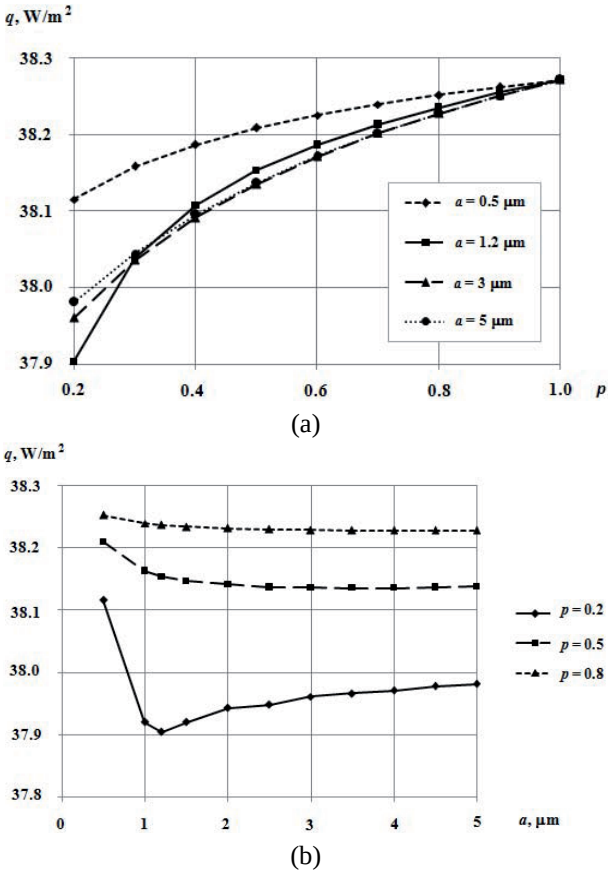

FIG. 5: Integral radiative flux as a function of **(a)** surface porosity and **(b)** fiber radius

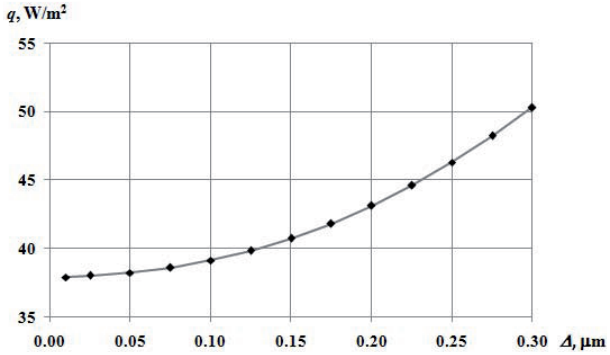

FIG. 6: Integral radiative flux as a function of the oxide film thickness at p = 0.2 and a = 1.2 μm

6. PERSPECTIVE OF FURTHER RESEARCH

An analysis of possible solutions for the fibrous spacer showed that the use of metalized quartz fibers may be a

very good choice to decrease the radiative flux without any increase in the MLI weight (the latter is very important for space vehicles). It was proven experimentally that layered materials made of dielectric fibers with a radius from 50 nm to 1.5 μm and aluminum coating 50 nm thick or even less are characterized by abnormally high attenuation of the infrared radiation (Ebert et al., 1991; Caps et al., 1993). The computational studies by Dombrovsky (1997, 1998) showed that the radiative properties of metalized fibers are very close to those of homogeneous metal fibers and can be estimated from the known solution for fibers made of a totally reflecting material. This dependence of the transport efficiency factor of extinction (or scattering) on diffraction parameter $x = 2\pi a/\lambda$ is shown in Fig. 7.

The great values of the transport extinction coefficient show that the hypothesis of independent scattering is true only for highly porous materials. Particularly, it was shown in Dombrovsky (1997, 1998) that the infrared properties of such materials are well predicted by the Mie theory at the volume fraction of fibers. More details about the spectral properties of metalized fibers including the effect of a thin oxide layer at the fiber surface can be found in Dombrovsky and Baillis (2010).

In the case of metalized fibers, the dependent scattering effects are expected to be significant at a surface density greater than about 0.5 (Tien and Drolen, 1987; Lee, 1996, 2011; Mishchenko et al., 2006). Of course, one cannot use the aforementioned approach to estimate the effect of a metalized spacer in the dependent scattering range. Instead, such a spacer can be approximately treated as an aluminum foil.

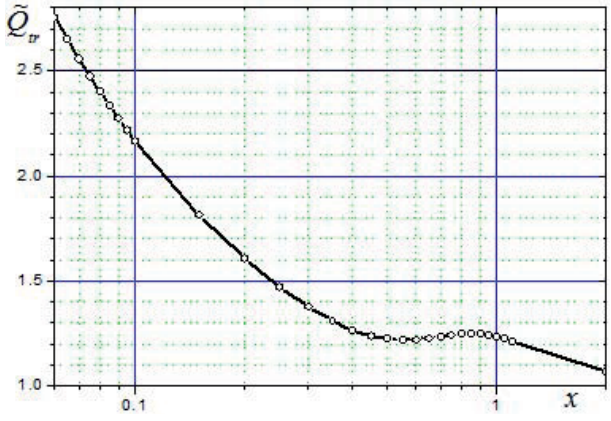

FIG. 7: Average transport efficiency factor of extinction for totally reflecting fibers randomly oriented in a normally irradiated layer

In this case, the ratio of radiative fluxes with and without the spacer is equal to

$$q_\lambda^{\rm sp}/q_\lambda = (1/\varepsilon_{1,\lambda} + 1/\varepsilon_{2,\lambda} + 2/\varepsilon_{{\rm sp},\lambda} - 2) \Big/ (1/\varepsilon_{1,\lambda} + 1/\varepsilon_{2,\lambda} - 1) \quad (15)$$

Neglecting the effect of temperature on aluminum foil emittance, one can find that this ratio is equal to 0.5. The above estimate of the maximum effect of a porous metalized spacer is very promising. Of course, the theoretical estimate is insufficient. Optical and thermal experimental studies should be done to optimize the parameters of the single metalized fibers and surface density of the spacer.

7. CONCLUSION

A novel radiative transfer model that takes into account a fibrous spacer and oxide film on the foil surface as applied to vacuum thermal insulations of space vehicles was developed. The calculations showed that the effect of ordinary highly porous spacers made of quartz fibers is very small and may be ignored in engineering calculations. The oxide film on aluminum foils at film thickness greater than about 1 μm should be taken into account. The upper estimates showed that a realistic spacer made of metalized fibers with aluminum coating about 50 nm thick may lead to an almost twofold decrease in the integral radiative flux. The latter is considered to be a promising direction for further experimental studies using both optical and thermal measurements.

ACKNOWLEDGMENTS

The authors are grateful to the Russian Foundation for Basic Research for the financial support of this study (Grant No. 13-08-00022-a). This work was also supported by the Russian Ministry of Science and Education in the frame of the Basic Part of the Government financial support.

REFERENCES

Alifanov, O. M., Nenarokomov, A. V., and Gonzalez, V. M., Study of multilayer thermal insulation by inverse problems method, *Acta Astronaut.*, vol. **65**, pp. 1284–1291, 2009.

Baetens, R., Jelle, B. P., Thue, J. V., Tenpierik, M. J., Grynning, S., Uvsløkk, S., and Gustavsen, A., Vacuum insulation panels for building applications: A review and beyond, *Energy Build.*, vol. **42**, no. 1, pp. 147–172, 2010.

Banner, D., Klarsfeld, S., and Langlais, C., Temperature dependence of the optical characteristics of semitransparent porous

media, *High Temp.–High Press.*, vol. **21**, no. 3, pp. 347–354, 1989.

Bartl, J. and Baranek, M., Emissivity of aluminium and its importance for radiometric measurements, *Meas. Phys. Quant.*, vol. **31**, no. 4, pp. 31–36, 2004.

Beder, E. C., Bass, C. D., and Shackleford, W. L., Transmissivity and absorption of fused quartz between 0.22μ and 3.5μ from room temperature to 1500°C, *Appl. Opt.*, vol. **10**, no. 10, pp. 2263–2268, 1971.

Bohren, C. F. and Huffman, D. R., *Absorption and Scattering of Light by Small Particles*, New York: Wiley, 1983.

Born, M. and Wolf, E., *Principles of Optics*, 7th Ed. (expanded), New York: Cambridge University Press, 1999.

Bouquerel, M., Duforestel, T., Baillis, D., and Rusaouen, G., Heat transfer modeling in vacuum insulation panels containing nanoporous silicas—A review, *Energy Build.*, vol. **54**, pp. 320–336, 2012.

Brannon, R. R. and Goldstein, R. J., Emittance of oxide layers on a metal substrate, *ASME J. Heat Transfer*, vol. **92**, no. 2, pp. 257–263, 1970.

Caps, R., Arduini-Schuster, M. C., Ebert, H. P., and Fricke, J., Improved thermal radiation extinction in metal coated polypropylene microfibers, *Int. J. Heat Mass Transfer*, vol. **36**, no. 11, pp. 2789–2794, 1993.

Chapius, P.-O., Volz, S., Henkel, C., Joulain, K., and Greffet, J.-J., Effect of spatial dispersion in radiative near-field radiative heat transfer between two parallel metallic surfaces, *Phys. Rev. B.*, vol. **77**, no. 3, p. 035431, 2008.

Dombrovsky, L. A., Radiative properties of metalized-fiber thermal insulation, *High Temp.*, vol. **35**, no. 2, pp. 275–282, 1997.

Dombrovsky, L. A., Infrared and microwave radiative properties of metal coated microfibers, *Rev. Geen. eTherm.*, vol. **37**, no. 11, pp. 925–933, 1998.

Dombrovsky, L. A., The use of transport approximation and diffusion-based models in radiative transfer calculations, *Comput. Therm. Sci.*, vol. **4**, no. 4, pp. 297–315, 2012.

Dombrovsky, L. A. and Baillis, D., *Thermal Radiation in Disperse Systems: An Engineering Approach*, Redding, CT: Begell House, 2010.

Ebert, H. P., Arduini-Schuster, M. C., Fricke, J., Caps, R., and Reiss, H., Infrared-radiation screens using very thin metallized glass fibers, *High Temp.–High Press.*, vol. **23**, no. 2, pp. 143–148, 1991.

Fricke, J., Heinemann, U., and Ebert, H. P., Vacuum insulation panels—From research to market, *Vacuum*, vol. **82**, no. 7, pp. 680–690, 2008.

Gritsevich, I. V., Dombrovsky, L. A., and Nenarokomov, A. V., Heat transfer by radiation in a vacuum thermal insulation of space vehicles, *Therm. Proc. Eng.*, vol. **5**, no. 1, pp. 12–21, 2013 (in Russian).

Gryvnak, D. A. and Burch, D. E., Optical and infrared properties of Al_2O_3 at elevated temperatures, *J. Opt. Soc. Am.*, vol. **55**, no. 6, pp. 625–629, 1965.

Howell, J. R., Siegel, R., and Mengüç, M. P., *Thermal Radiation Heat Transfer*, Boca Raton, FL: CRC Press, 2010.

Kitamura, R., Pilon, L., and Jonasz, M., Optical constants of silica glass from extreme ultraviolet to far infrared at near room temperatures, *Appl. Opt.*, vol. **46**, no. 33, pp. 8118–8133, 2007.

Kralik, T., Hanzelka, P., Zohac, M., Musilova, V., Fort, T., and Horak, M., Strong near-field enhancement of radiative heat transfer between metallic surfaces, *Phys. Rev. Lett.*, vol. **109**, no. 22, p. 224302, 2012.

Lee, S.-C., Radiative transfer through a fibrous medium: Allowance for fiber orientation, *J. Quant. Spectrosc. Radiat. Transfer*, vol. **36**, no. 3, pp. 253–263, 1986.

Lee, S.-C., Radiation heat-transfer model for fibers oriented parallel to diffuse boundaries, *AIAA J. Thermophys. Heat Transfer*, vol. **2**, no. 4, pp. 303–308, 1988.

Lee, S.-C., Angle of incidence and size effects on dependent scattering in fibrous media, *ASME J. Heat Transfer*, vol. **118**, no. 4, pp. 931–936, 1996.

Lee, S.-C., Wave propagation through a dielectric layer containing densely packed fibers, *J. Quant. Spectrosc. Radiat. Transfer*, vol. **112**, no. 1, pp. 143–150, 2011.

Lee, S.-C. and Cunnington, G. R., Theoretical models for radiative transfer in fibrous media, *Annual Review in Heat Transfer*, C. L. Tien, ed., vol. **9**, pp. 159–218, New York: Begell House, 1998.

Lingart, Yu. K., Petrov, V. A., and Tikhonova, N. A., Optical properties of synthetic sapphire at high temperatures. II. Properties of monocrystal in opacity region and melt properties, *High Temp.*, vol. **20**, no. 6, pp. 1085–1092, 1982.

Malozemov, V. V., Rozhnov, V. F., and Pravetski, V. N., *Life-Support Systems for Space Crews*, Moscow: Mashinostroenie, 1986 (in Russian).

Mishchenko, M. I., Travis, L. D., and Lacis, A. A., *Multiple Scattering of Light by Particles: Radiative Transfer and Coherent Backscattering*, New York: Cambridge University Press, 2006.

Nenarokomov, A. V., Alifanov, O. M., and Gonzalez, V. M., Identification of mathematical model of multilayer thermal insulation, *Proc. of 6th International Symposium on Radiative Transfer*, Antalya, Turkey, June 13–19, 2010.

Ordal, M. A., Long, L. L., Bell, R. J., Bell, S. E., Bell, R. R., Alexander, R. W., Jr., and Ward, C. A., Optical properties of the metals Al, Co, Cu, Au, Fe, Pb, Ni, Pd, Pt, Ag, Ti, and W in the infrared and far infrared, *Appl. Opt.*, vol. **22**, no. 7, pp. 1099–1119, 1983.

Parka, K. and Zhang, Z., Fundamentals and applications of near-field radiative energy transfer, *Front. Heat Mass Transfer*,

vol. **4**, no. 1, p. 013001, 2013.

Sokolov, A. V., *Optical Properties of Metals*, Moscow: Fizmatgiz, 1961 (in Russian).

Tan, C. Z. and Arndt, J., Temperature dependence of refractive index of glassy SiO_2 in the infrared wavelength range, *J. Phys. Chem. Solids*, vol. **61**, no. 8, pp. 1315–1320, 2000.

Tien, C. L. and Drolen, B. L., Thermal radiation in particulate media with dependent and independent scattering, *Annual Review of Numerical Fluid Mechanics and Heat Transfer*, vol. **1**, pp. 1–32, New York: Hemisphere, 1987.

Whitson, M. E., *Handbook of the Infrared Optical Properties of Al_2O_3, Carbon, MgO and ZrO_2*, vol. **1**, El Segundo, CA: Aerospace Corporation, 1975.